Ardestani *et al. Chem. Biol. Technol. Agric.* (2022) 9:83
https://doi.org/10.1186/s40538-022-00355-7

Chemical and Biological Technologies in Agriculture

RESEARCH Open Access

Phase separation and formation of sodium caseinate/pectin complex coacervates: effects of pH on the complexation

Faezeh Ardestani[1], Ali Haghighi Asl[1*] and Ali Rafe[2*]

Abstract

Background: The electrostatic interactions between polysaccharides and proteins are an interesting field in the complex coacervation. PH and mixing ratio have major effect on the complexation and the coacervates structure. Hence, it is necessary to find the optimum pH and mixing ratio of the coacervates as well as understanding the thermal, mechanical, and structural characterization of the coacervates. Thus, structural changes of the complexes of sodium caseinate (NaCas) and high methoxyl pectin as a function of pH (2.00–7.00), biopolymer ratios (1:1, 2:1, 4:1, and 8:1), and total biopolymer concentration (0.1, 0.2, and 0.4% *w/v*) were evaluated by light scattering and ζ-potential measurements. The phase separation behavior of the NaCas/HMP coacervate and its kinetics turbidity were also investigated via monitoring the turbidity profiles. Moreover, the thermal, rheological and structural behavior of the coacervates was evaluated at the selected pH values.

Results: The highest turbidity, particle size, and viscosity were achieved at $pH_{max} = 3.30$ and formation or dissociation around the pH_{max} was confirmed by particle size and FTIR. The optimum condition for the coacervation of NaCas and HMP was obtained at ratio 4:1 and 0.4% *w/v*. Thermal and mechanical stability of the NaCas/HMP coacervates was improved at pH 3.30. By increasing the total concentration of biopolymers, the NaCas/pectin ratio shifted to higher pH values. Furthermore, the maximum coacervate yield was achieved at 39.8% w/w at a ratio of 4:1 of NaCas/HMP and a total biopolymer concentration of 0.4% *w/v*.

Conclusion: Phase separation behavior of the coacervates exhibited the optimum pH in coacervation between NaCas and HMP. Furthermore, the rheological, thermal and structural stability of the coacervates were improved in comparison with the single biopolymers.

Keywords: High methoxyl pectin, Caseinate, Complex coacervation, Electrostatic interactions, Turbidity

*Correspondence: ahaghighi@semnan.ac.ir; a.rafe@rifst.ac.ir

[1] Faculty of Chemical, Petroleum and Gas Engineering, Semnan University, 3513119111, Semnan, Iran
[2] Department of Food Processing, Research Institute of Food Science and Technology (RIFST), 91775-1163, Mashhad, Iran

Graphical Abstract

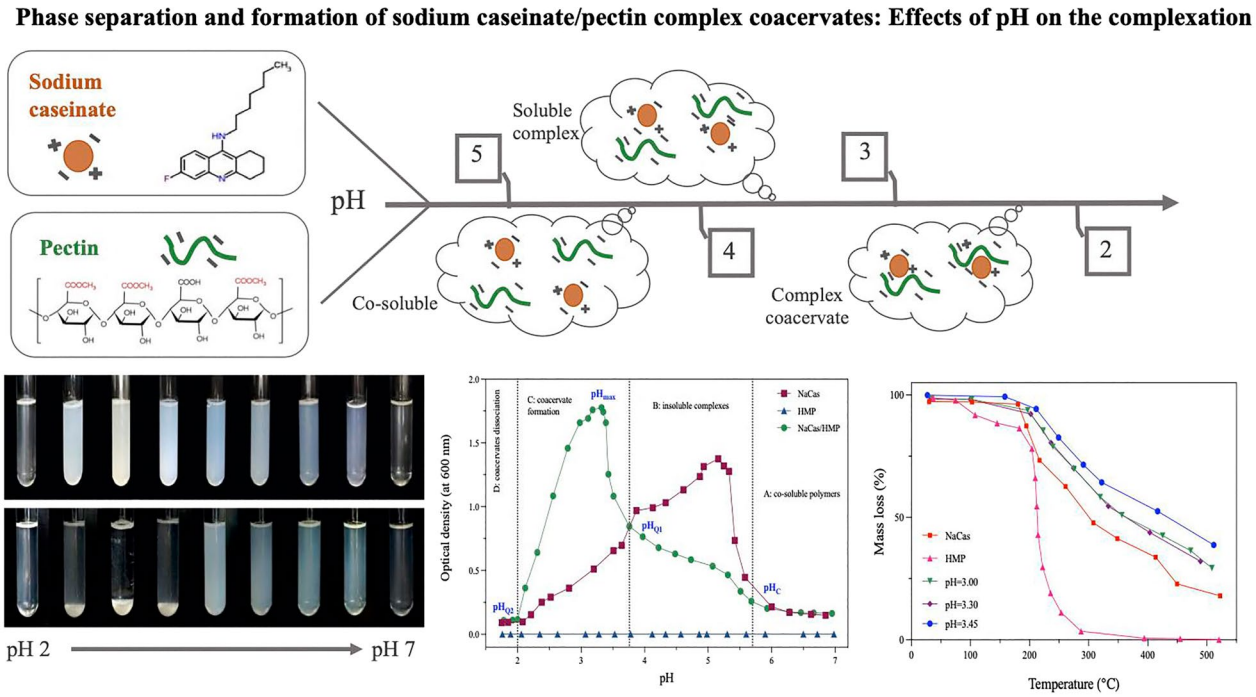

Introduction

Polysaccharides and proteins are natural biodegradable polymers with large molecular structures, which have a significant effect on the structure, texture, and stability of foods. Due to their excellent biological properties, such as non-toxicity, biocompatibility, and biodegradability, they are widely used in the food industry. In addition, they are used as biomaterials, e.g., for structural control, controlled release, stabilization, coating, and packaging of foods and pharmaceuticals [1–4]. In recent years, studies have focused primarily on protein/polysaccharide complexes formed by electrostatic interactions between oppositely charged biopolymers. In an aqueous solution, they can interact through electrostatic forces, hydrogen and hydrophobic bonds to form either soluble complexes or coacervates depending on several intrinsic or extrinsic factors, such as the charge of the biopolymer and the medium conditions [5]. This complexation initiates spontaneous phase separation, called complex coacervation (CC) [2, 6].

Coacervation often occurs in systems containing two or more biopolymers. The anionic groups of the polysaccharides interact with the net positive charge of the proteins at pH values lower than the isoelectric point (*IP*). Direct interactions of protein/polysaccharide complexes at a given pH or adsorption of ionic polysaccharides onto preformed protein particles initiate complex formation. Consequently, one phase is rich and dense in biopolymers, while the other contains a smaller amount of coacervates and is referred to as the supernatant [7–10]. It has been shown that both intrinsic properties of the biopolymers, i.e., molecular weight, charge density, concentration, and mixing ratio, and extrinsic factors, such as temperature, ionic strength, and pH, influence coacervation [11, 12]. Coacervation has also found various applications in living cells, encapsulation of bioactive materials, purification, stability improvement, texture, and pharmaceutical industry [2, 7, 13]. Further perception of biopolymer factors and interactions leading to their phase behavior can enhance their application in modifying food structures or developing high-value-added products, such as capsules, films, etc. [1].

Sodium caseinate (NaCas) is a water-soluble polymer with a random-coil structure which contains four types of phosphoproteins, including α_{s1}-, α_{s2}-, β-, and κ-caseins. Its ability to form molecular interactions (hydrogen, hydrophobic, and electrostatic), depending on pH, makes it an excellent candidate for producing coacervates [5, 14]. Numerous studies have concentrated on improving the multifunctionality of caseins by modifying them

through physical, chemical, and biochemical methods and mixing them with other biopolymers. Moreover, several investigations have tried to avoid precipitation of the casein micelles in the acidic dairy drinks. It has been understood that polysaccharide addition leads to phase stabilization, which depends entirely on pH [5, 15].

High methoxyl pectin (HMP) is an anionic polysaccharide compound made from a linear chain of the units of galacturonic acid joined via α-1-4 links, interspersed via rhamnose units linked via α-1-2, in which methyl groups may esterify the carboxylic groups of the galacturonic acid. Due to its low cost and high occurrence, it offers unique technological properties in food applications [4, 10, 14]. Moreover, HMP and its derivatives are used in the food and pharmaceutical industries due to their gelling, thickening, packaging, and stabilizing properties [5, 15]. It has been shown that the development of NaCas/HMP complexes is highly dependent on the pH value. Since NaCas has many cationic groups and HMP has anionic properties at low pH, the highest interactions occur at pH 3.00 to 5.50. However, the electrostatic NaCas/HMP interactions can form insoluble and soluble complexes at different pH values [1, 16].

Despite the wide range of proposed applications for the use of coacervates in the food and pharmaceutical industries, the optimum conditions for preparation of the NaCas/HMP complexes, including the effects of pH on the formation of CC and their functional properties, are not prevalent in the literature. The pH and mixing ratios are expected to influence the complexation thereby affecting the coacervates structure. Hence, it should be possible to optimize the conditions for the preparation of the coacervates as well as improve their thermal and rheological properties by structural changes of the electrostatic complexes. Therefore, the main objective of the work was to create NaCas/HMP coacervates as a function of pH and to evaluate their structural, thermal, and rheological properties. The interaction between NaCas and HMP was investigated through measuring optical density and ζ-potential. FTIR, TGA, DSC, and optical microscopy were performed to recognize the behavior of coacervate at selected pH values. Furthermore, the turbidity kinetics of the NaCas/HMP coacervates was carefully studied as a function of pH. Our findings open new horizons in phase behavior between NaCas and HMP and extend their application in food and pharmaceutical industries (e.g., controlled release and encapsulation of bioactive compounds).

Materials and methods

Materials

Sodium caseinate (NaCas) from bovine milk (protein content higher than 97%) and high methoxyl pectin (Galacturonic acid content >74%, molecular weight 131 kDa) were obtained from Sigma-Aldrich Chemical Co. (Saint Louis, MO, USA). Sodium hydroxide (NaOH), hydrochloric acid (HCl), and other chemicals consumed were analytical grades purchased from Merck Company (Merck Company, Darmstadt, Germany).

Sample preparation

The stock protein solution was prepared by slowly dispersing the appropriate amount of protein (0.5% *w*/*v*) in distilled water with continuous stirring for at least 3 h at ambient temperature. The HMP stock solution (0.5% *w*/*v*) was also prepared via slow addition of HMP into deionized water and kept stirring for more than 2 h. Both solutions were kept overnight in the refrigerator (4 °C) to finalize hydration. To avoid microbial growth, 0.02% (*w*/*v*) sodium azide was added to both stock solutions.

Using the prepared stock solutions, mixtures of NaCas and HMP were prepared with different proteins: polysaccharide ratios (i.e., 1:1, 2:1, 4:1, and 8:1) and total biopolymer concentrations ($C_T = 0.1$, 0.2, 0.4, 0.6, and 0.8% *w*/*v*). For the NaCas/HMP mixtures, the pH was also modified by dropwise addition of HCl or NaOH (0.01, 0.1, and 1 M), ranging from 2.00 to 7.00.

Turbidity measurement

Optical density was monitored in a pH range from 2.00 to 7.00 by determining absorbance at 600 nm via a UV–visible spectrophotometer (UV-1800, Shimadzu, Hitachi, Japan). For time-dependent turbidity measurements, a cuvette was filled with 3 ml of the NaCas/HMP mixture, and the turbidity was recorded with a measuring step of 30 s for 20 min. The following equation defines the turbidity (T, cm^{-1}) [17]:

$$T = -\left(1/L\right) \ln\left(I/I_0\right) \quad (1)$$

where L represents the light path length (1 cm), I stands for the light intensity on the detector when the sample is present, and I_0 stands for the light intensity of distilled water. All samples were measured at least 3 times at ambient temperature. The crucial pH values to form soluble complexes of NaCas/HMP (pH_c), insoluble complex coacervates ($pH_{\phi 1}$), and dissolution of complex coacervates ($pH_{\phi 2}$) were graphically determined as the intersection of two curve tangents on the turbidity–pH curves [18].

ζ-Potential measurements

The average surface electrical charge (ζ-potential) of the samples was determined using a Malvern Nano Zetasizer (Malvern Instruments Ltd., United Kingdom) with

a U-shaped cuvette. According to the results of turbidity measurements, the NaCas/HMP mixture at a ratio of 4:1 (0.32% *w*/*v* NaCas and 0.08% *w*/*v* HMP) was selected for the test. Fresh samples were measured in ten repetitions at ambient temperature, and the mean ζ-potential values were reported.

Particle size analysis

The particle size of NaCas/HMP coacervates (Ratio = 4:1, C_T = 0.4% *w*/*v*) was determined via the dynamic light scattering (DLS) technique (Malvern, Worcestershire, UK). The temperature of the cell was kept at 25 °C during the experiments. The experiment was carried out using a refractive index of 1.57, and the "fine particle" mode was activated to improve the measurement. The mean diameters of the complexes were stated as volume mean diameter (d_{43}) using the Mie Theory. The measurements were carried out with five repetitions.

Fourier transform infrared spectroscopy (FTIR)

The NaCas/HMP coacervate samples were centrifuged and freeze-dried (FD-8505/FD-5005-BT freeze dryer, Dena Vacuum Industry Co., LTD, Tehran, Iran) for further application. The FTIR spectra of NaCas, HMP, and freeze-dried NaCas/HMP coacervates were performed by the Shimadzu FTIR-8400S spectrometer (Kyoto, Japan), a double beam spectrometer with the KBr pellet in the range of 400–4000 cm^{-1} at room temperature (~ 23 ± 0.5 °C) and a resolution of 4 cm^{-1} was used. The infrared spectrum of pure KBr was selected as a baseline, and the details of the FTIR method have been described in our previous work [19]. All the experiments were carried out in three replicates.

Thermal characterization

Thermal analysis of NaCas, HMP, and freeze-dried NaCas/HMP coacervates were investigated by the simultaneous thermal analyzer (Bähr-Thermoanalyse GmbH, Hüllhorst, Germany) under the argon atmosphere at a steady airflow. A certain amount of the samples was heated from 20 to 520 °C at 10 °C/min. Meanwhile, the samples were measured by a DSC (Sanaf DSC/OIT measurement, Tehran, Iran). The samples (25–30 mg) were loaded into an aluminum pan, hermetically sealed, and scanned over a temperature range from 20 to 350 °C with a heating rate of 10 °C/min in a nitrogen atmosphere.

Rheological properties

The apparent viscosities of NaCas (0.32% *w*/*v*), HMP (0.08% *w*/*v*), and the mixture of NaCas/HMP at a ratio of 4:1 and different pH values including 3.00, 3.30 and 3.45 were prepared freshly and measured by a rotary digital viscometer (Brookfield DV3T LV, Brookfield Co., USA). The temperature was controlled with a constant temperature bath at 25 °C. The apparent viscosities of NaCas and HMP were measured at pH = 5.00. The spindle ULA (ULA-DIN-85, sample volume 16 mL), suitable for low viscosity fluids, was utilized. An aliquot of 16 mL was added into the container with a thermal jacket connected to the rheometer. The viscosity of the sample was fixed by changing the spindle rotational speed. The spindle rotational speed produced satisfactory results when the applied torque was in the range of 0.1–100%. The measurement accuracy of the device was predicted at 1%.

Light microscopy

The NaCas and HMP at pH = 5.00, and NaCas/HMP mixture at different pH values including 3.00, 3.30, and 3.45 were slowly shaken in a plastic test tube before the assay to provide a homogeneous sample to ensure homogeneity. A drop of the mixtures was placed on a glass microscope slide, then covered by a coverslip and allowed to air-dry. It was observed using a Fluorescence microscope (OPTEC BK5000-FL, Drawell, Shanghai, China) at a magnification of 40×.

Complex coacervation yield

The aqueous solutions of NaCas/HMP at varying mass ratios (2:1, 4:1, and 8:1) and different C_T (0.1, 0.2, and 0.4% *w*/*v*) were prepared at room temperature to determine the yield of the coacervation. The pH was adjusted to the optimum, which was determined via the outcomes of turbidity and zeta-potential. The NaCas/HMP coacervates precipitated at the bottom of the tubes, and then they were maintained at 4 °C for 24 h for stabilization. The precipitated coacervates were recovered from the equilibrium phase by centrifugation (at 8500 rpm for 10 min) and subsequently dried in an oven at 60 °C, till achieving a constant weight. The yield of the coacervate was calculated according to our previous work [20, 21] using the following equation:

$$\text{Coacervate yield } \% = \left[{}^{m}/_{(m_{\text{NaCas}} + m_{\text{HMP}})} \right] \times 100\% \quad (2)$$

where m stands for the total mass of dried NaCas/HMP coacervates, m_{NaCas} and m_{HMP} are the masses of NaCas and HMP, respectively. The entire experiments were conducted in triplicate.

Statical analysis

Unless otherwise stated, the entire tests were conducted at least in triplicates. The obtained data were analyzed using SPSS and GraphPad, Prism. All the data

were expressed as the mean ± standard deviation. Furthermore, a one-way analysis of variance (ANOVA) was applied with a 95% significance level ($P < 0.05$) to show the significant difference among the samples at different pH values for the particle size and yield of complex coacervation.

Results and discussion

Turbidity kinetic of the NaCas/HMP coacervate

Although turbidimetry is one of the most important procedures in the study of coacervation, it is still applied to investigate the relationship between intrinsic/exogenous factors due to its intuitive and convenient nature. The

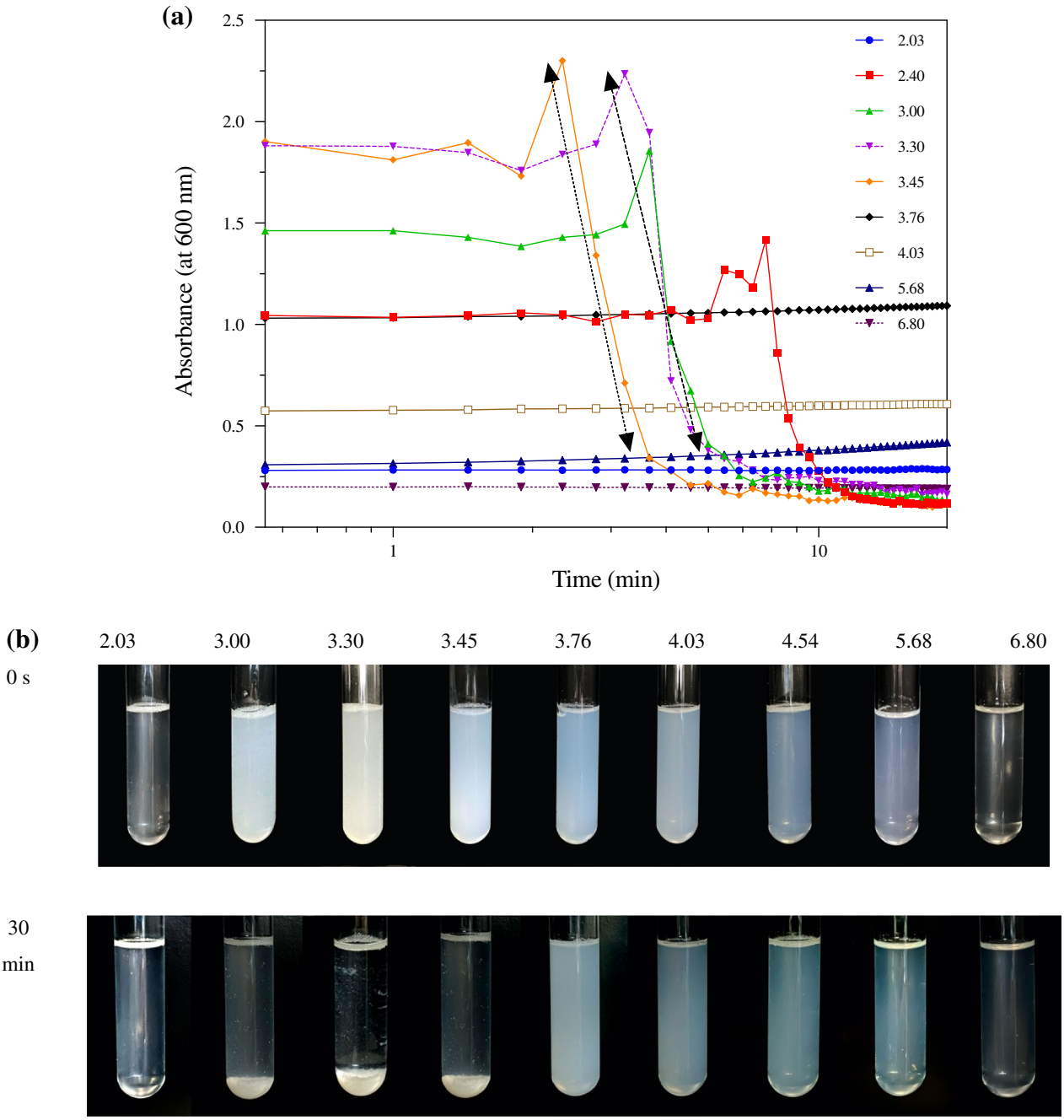

Fig. 1 Changes in the turbidity of NaCas/HMP mixtures observed over time. **a** Optical density of NaCas/HMP mixtures at ratio = 4:1, and total biopolymer concentration = 0.4% *w/v* as affected by varying pH values in semi-logarithmic scale (Arrows shows the reduction percentage of the turbidities). **b** Images of NaCas/HMP mixtures as a function of pH, at the beginning of dissolution and after 30 min

kinetics study of turbidity, that reflects changes in turbidity as a function of time, demonstrates the alterations in the early and mid-term of CC [22–26]. Therefore, turbidity kinetics of NaCas/HMP mixtures ($C_T = 0.4\%$ *w*/*v*, R = 4:1) at different pH values was evaluated by turbidity measurement for 20 min (Fig. 1a). Furthermore, the stability of the mixtures for half an hour in the glass tubes is provided in Fig. 1b.

As expected, at pH = 6.80, the solution is crystal clear, which can be attributed to negatively charged biopolymers hindering their complexation (Fig. 1a). By further pH reduction (pH 5.68–4.03), the turbidity of the NaCas/HMP increased. In contrast, the mixture at pH 5.68–4.03 displayed no macroscopic phase separation, revealing some attractive interactions between the NaCas and HMP. Due to their high remaining charges, these soluble intra-polymeric complexes were entirely stable [27]. To ensure the stability of mixtures, the solution was kept at pH of 5.68 and 4.03 for 20 min, although the turbidity at pH 4.03 remained entirely constant, the turbidity was slightly increased at pH 5.68 (Fig. 1a). In addition, no phase separation took place at the pH range from 5.68 to 3.76 (Fig. 1b), indicating turbidity did not depend on time. Such stability can be explained by considering pure negative charges on the cited complexes supplying an effective electrostatic repulsion between assemblies that causes solution stability during the period of time [20, 28]. At pH = 3.45, macroscopic phase separation occurred, denoting the beginning of the phase separation and the formation of insoluble complexes (Fig. 1b). The same pH triggered the launch of phase separation.

The comparison of the reduction percentage for the turbidities at $t = 0$ s and 20 min for each pH indicates that the higher slope of the turbidity decrement led to higher rates of phase separation. The turbidity declined with a steeper slope throughout the storage time (20 min, Fig. 1a), revealing the phase separation took place at a faster rate. For instance, at pH = 3.45, the percentage of turbidity reduction approached to 89.11% in the initial 5 min, while it was reached to 53.77% at pH = 3.00. Earlier investigations have found that more vital electrostatic interactions are the cause of faster phase separation [29].

In the upper phase, turbidity is associated with the creation of a non-soluble phase that may precipitate or remain stable for a short time. This result connotes that, at the end of 30 min, solutions with increased turbidity have a very high number of macromolecules in the upper phase compared to the transparent solutions. Due to the stable and more soluble complexes found in the upper phase at pH = 3.76, greater turbidity was noted after 30 min. At pH = 3.00 (Fig. 1b), lower turbidity was observed, which may be attributed to the creation of more insoluble aggregates. Therefore, fewer soluble complexes were present in the upper phase. During the 30 min, the mixed dispersion (pH 6.80–4.03) illustrated comparatively constant and low turbidity. At the same pH values, due to their more residual charges, which supply effective electrostatic repulsion, soluble intra-polymeric complexes were utterly stable. At pH = 3.30, the highest transparency of the upper phase compared to the other pH values was realized after 30 min, which may demonstrate less formation of the soluble complexes and more insoluble aggregates. The results (Fig. 1b) provide a clear explanation of the dissociation of complexes, which are inclined to boost a single phase at shallow values of pH (pH = 2.03). As a consequence, this simple method can demonstrate the coacervate systems' stability and the different stages in CC.

Formation of NaCas/HMP coacervates.

HMP is an anionic polysaccharide with negative surface charges, while NaCas, which has an isoelectric point (*IP*) of 4.6, gets protonated at lower pH's and carries positive charges at the pH below their *IP*. Therefore, an effective means to acquire suitable interactions between them is the pH of the solution. Depending on the intensity of electrostatic interactions, either soluble or insoluble complexes would exist. At this condition, the protein and polysaccharide can conjugate through covalent bonds and, or physical interactions, such as electrostatic, hydrophobic, steric, hydrogen bonding, etc. [30], which provides some functional structures in food and pharmaceutical applications.

By measuring absorbance, structural transitions through the electrostatic interactions between NaCas and HMP during acidification were examined. Therefore, the turbidity curves of NaCas, HMP, and NaCas/HMP mixture (R = 4:1 and $C_T = 0.4$), as a function of pH are presented in Fig. 2. Four distinct regions revealed the development of different complex structures. The critical pH transitions, including pH_c, $pH_{\phi 1}$, and $pH_{\phi 2}$ were determined through the intersection point of the two curve tangents. The primary co-soluble complexes between the biopolymers are observed at $pH_c = 5.70$. Here, the NaCas and HMP have negative charges, which form co-soluble polymers. Theoretically, the protein has a negligible charge (*IP* = 4.6) at pH = 5.70 which could not permit complexation with polysaccharide chains. Nonetheless, the weak interactions between patches localized on NaCas molecules with positive charges and negatively charged carboxyl groups of the HMP backbone can justify the formation of small soluble complexes [1, 15, 31]. When pH surpasses the *IP* of the protein, some NaCas molecules' moieties are still positively charged. The same patches featuring positive charges may interact with polysaccharides with negative charges (negative carboxyl

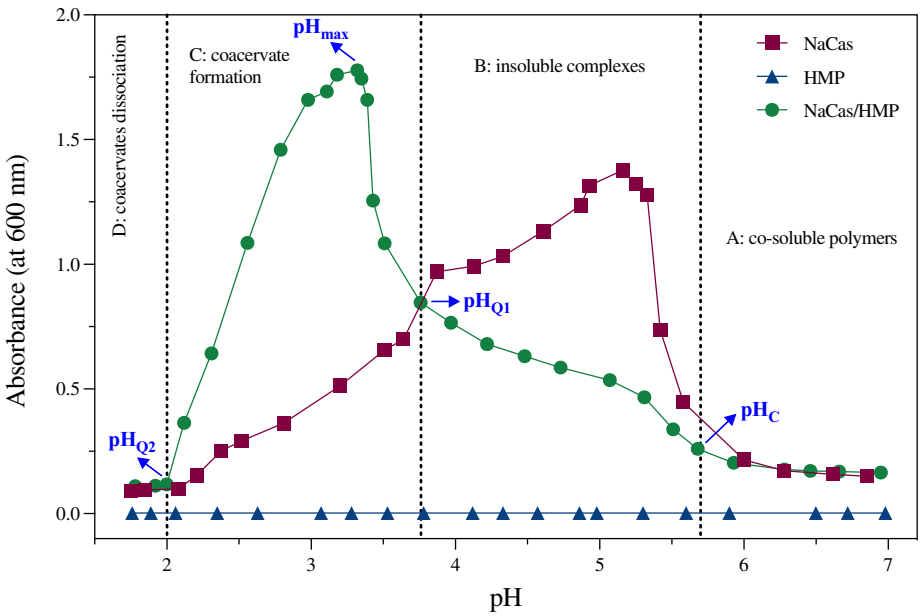

Fig. 2 Turbidity of NaCas (0.32% *w/v*), HMP (0.08% *w/v*), and NaCas/HMP solutions as a function of pH. The conditions for NaCas/HMP mixture were: biopolymer mixing ratio R = 4:1, C_T = 0.4% *w/v*, and ambient temperature. The structure development of soluble (pH_c), insoluble ($pH_{\varphi 1}$) complexes, the coacervate formation (pH_{max}), and dissociation of complex coacervate ($pH_{\varphi 2}$) are provided

groups), so that soluble complexes are formed, which can reveal the fact that pH_c surpassed the protein *IP* [1].

With a further reduction in pH to 3.76 ($pH_{\phi 1}$), the same soluble complexes that are incompletely neutralized may attract other molecules of NaCas, which leads to the formation of more detectable insoluble complexes of greater size, so that a swift increase in turbidity was observed. The electrostatic interactions between NaCas and HMP molecules with opposite charges are increased, which is evidenced by the transition from a transparent state to a cloudy state with perspectives of macroscopic phase separation, similarly found for casein/κ-carrageenan, gelatin/pectin, and lysozyme/pectin [32–34]. The turbidity will achieve its highest value at pH_{max} = 3.30 by further acidification when the charge neutrality, highest intermolecular interactions, and coacervation occur. Due to the negative charge of HMP and the positive charge of NaCas surface at pH_{max} (< *IP*), electrostatic interactions can be considered as the main driving force [8, 12]. This trend could be observed when the net charge of NaCas and HMP became opposite and, at pH_{max}, reached an electrical equivalence [35]. At pH < 2.00 (< pKa = 2.80), HMP became highly protonated, leading to coacervate dissociation, in which the mixture was more transparent and absorbance was reduced ($pH_{\phi 2}$). At this phase, the coacervates dissociation as an attractive interaction is reduced due to the same net charge of individual biopolymers [12, 14, 36, 37].

In comparison with coacervates, NaCas and HMP solutions showed lower turbidity than their mixtures by pH reduction. As a function of pH, the turbidity of HMP was negligible and did not alter, which has been similarly observed by various researchers [26, 27]. As illustrated in Fig. 2, the turbidity of NaCas solution remained unchanged until it reached a pH = 6.00. Turbidity climbed to the peak at pH = 5.16, and then, as pH increased to the acidic range, it fell back to lower values. This approves that the NaCas solubility is pH-dependent [27, 38]. The increment in turbidity is mainly attributed to the increase in particle size and number of particles [39]. On the contrary, turbidity reduction is presumed to be a result of large-scale aggregation followed by precipitation of NaCas. Indeed, the solution featured two phases, i.e., the transparent supernatant phase and the sedimented protein particles. Aggregation of the NaCas can result from a decrease in the electrostatic repulsion between proteins around their *IP* [40]. A combination of van der Waals, hydrophobic, and several electrostatic attractions may be responsible for protein aggregation near the *IP*. Moreover, below *IP* of protein (further acidification) could create more positive charges on the NaCas that could lead to the increase in the solubility of the protein and consequently a decrease in the turbidity of the system [41].

The magnitude of turbidity of the protein/polysaccharide mixture in dilute suspension, which is mainly

affected by the size and concentration of the particles, can be considered a sign of complex formation or dissociation [34, 37]. The Veis-Aranyi theory developed by Tainaka can be described as the existence of two steps in the mechanism of interaction between NaCas and HMP. According to this theory, the spontaneous aggregation of biopolymers with opposite charges occurs in the first step due to electrostatic interaction, forming aggregates of low configurational entropy. The coacervate phase is formed through the slow rearrangement of these aggregates. Rearrangement is done by incrementing configurational entropy [42]. In this process, pH plays a critical role in determining the strength of electrostatic interactions, which dramatically affect the CC between two biopolymers [8, 43]. Therefore, it is suitable to optimize pH for the best possible coacervate formation between NaCas and HMP.

ζ-Potential

Electrophoretic mobility of a polymer can be determined by ζ-potential, which is mainly influenced by the pH of a solution [8, 12, 44]. The ζ-potential of HMP, NaCas, and NaCas/HMP solutions at a ratio of R = 4:1 and $C_T = 0.4\%$ *w*/*v* as a function of pH is provided in Fig. 3. It can be understood that the changes made by NaCas in the electrical charge of the proteins from the negative charge of − 27.34 ± 0.71 mV at pH = 8.00 to the positive charge of 27.01 ± 0.83 mV at pH = 3.00 with an approximate zero load point (*IP*) of 4.6 as previously reported [45]. The negativity of NaCas increased incrementally with pH, and at pH = 6.0, the ζ-potential of NaCas solution increased to − 19.86 ± 0.71 mV, which has been similarly found in the literature [4]. Under the same circumstances, the micelles of NaCas remain in suspension as a result of electrostatic and steric repulsions between hairy NaCas layers [15]. Further acidification was accompanied by a decrease in ζ-potential of up to − 9.895 ± 0.54 mV, and when the value of pH advanced toward the *IP* of protein, ζ-potential became positive. This reduction in ζ-potential can be attributed to the increased number of carboxyl groups with a negative charge (–COO) and the increased number of neutralized amino groups ($–NH_2$) upon the pH increase [20].

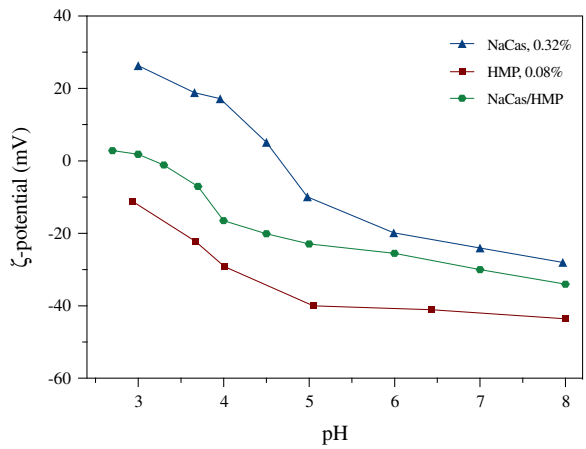

Fig. 3 ζ-Potential of NaCas, HMP and NaCas/HMP mixture at R = 4:1 and $C_T = 0.4\%$ *w*/*v*, depending on pH value (temperature 25 °C)

As demonstrated in Fig. 3, due to its carboxyl-based anionic polysaccharide backbone, HMP retained the negative charge at entire values of pH [46]. As expected, HMP addition to NaCas solutions at different ratios could affect the net electrical charges of micelles. Typically, at neutral pH values, HMP does not make complexes with micelles of NaCas due to the repulsive forces developed by the same negative charges [15]. Indeed, as a result of carboxyl groups' deprotonation, the negative charge of HMP increases significantly [14, 46, 47]. Nevertheless, NaCas features two opposite charges on one side and another one of the *IP* (~4.6) (at pH < 4.60, below its isoelectric point, NaCas features a positive surface charge). It means that the number of NH_3^+ groups surpasses that of the carboxyl groups (− COOH), and the overall charge of NaCas remains positive [20, 44].

In the NaCas/HMP mixture, the decline of pH from 5.00 to 4.00 did not result in significant changes in ζ-potential, so that it remained at an approximate value of − 22.9 ± 0.71 mV. From pH = 4.00 downward, ζ-potential increased at a rapid rate as pH declined. The turning point remained close to the NaCas *IP*. As aforementioned, the positively charged patches of NaCas molecules interacted with negatively charged segments of the HMP molecules, leading to the coacervate development, which clearly implies the electrostatic interactions between carboxyl groups of the HMP and amino groups of the protein. The same result revealed that when two biopolymers with opposite charges form complexes, ζ-potential was subject to dramatic changes. Nonetheless, the ζ-potential was not subject to substantial changes for two biopolymers carrying identical charges (pH > 5.00). In case where the approximate value of ζ-potential of the complexes was zero, namely, the complexes featured a neutral electrical charge, coacervation was maximized. Soluble complexes were formed in case of relatively high net charges (the ζ-potential was about > − 22.9 ± 0.71 mV). It indicates quite strong electrostatic interactions as well. By reduction of pH via decreasing the net charge of complexes, CC takes place, resulting in phase separation.

Particle size analysis

Particle size distribution is widely applied to monitor the growth and formation of electrostatic complexes between

Table 1 *Z*-average and poly dispersity index (PDI) of HMP/NaCas at R = 4:1 and C_T = 0.4% *w/v* as functions of pH*

pH values	*Z*-average (μm)	PDI
2.70	9.963 ± 1.267^{c}	0.408 ± 0.107^{c}
3.00	12.918 ± 2.483^{b}	0.348 ± 0.207^{d}
3.30	33.212 ± 12.825^{a}	0.589 ± 0.380^{a}
3.70	6.237 ± 0.528^{d}	0.490 ± 0.146^{b}
4.00	0.391 ± 0.007^{e}	0.264 ± 0.034^{e}
4.50	0.289 ± 0.008^{f}	0.233 ± 0.036^{e}
5.00	0.295 ± 0.005^{f}	0.255 ± 0.016^{e}

* Alphabetic letter was used to show the significant difference among the sample ($P < 0.05$)

polysaccharides and proteins [27]. Therefore, it was used to evaluate the formation of NaCas/HMP complexes at different pH values [48–50]. Particle size was determined for the CC at R = 4:1 and varying pH values. The *z*-average and polydispersity index (PDI) of HMP/NaCas at R = 4:1 as functions of pH are provided in Table 1. The maximum particle size and PDI was achieved for the samples at pH 3.30 ($P < 0.05$). At all pH values, since there is a polydisperse system, the function can no longer be represented as a single exponential decay and must be represented as an intensity-weighed integral over a distribution of decay rates and should be normalized. The micelles of casein showed a hydrodynamic radius of about 12 nm, a radius of gyration of approximately 8.3 nm, and an interaction radius of approximately 15 nm at pH > 5.5. Furthermore, HMP indicated a hydrodynamic radius of about 3.7 nm.

The size of the NaCas/HMP complex at pH = 5.00 was 0.295 ± 0.0054 μm. The interactions observed between NaCas and HMP molecules have been formerly reported at pH values somewhat above the *IP* of the adsorbed protein layer, even though both molecules of NaCas and the HMP feature have a net negative charge. In the same limited pH area, the groups with a negative charge located on the molecules of HMP are attached to groups with a positive charge, located on the surfaces of proteins, provided the electrostatic repulsions created between the droplet surfaces and HMP molecules are not that large to stop them from reaching the proximity of each other [16]. With a further decrease of pH, the size of NaCas/HMP coacervate was changed to 0.289 ± 0.0084 μm and 0.391 ± 0.0077 μm for pH 4.50 and 4.00, respectively. The particle sizes in many coacervates increased significantly when the pH declined ($P < 0.05$), ascribable to the flocculation of droplets caused by the bridging effect or charge neutralization [16]. At pH = 3.70, the particle size increased to 6.2 ± 0.52 μm. It was in agreement with the formation of insoluble complexes that reached their maximum intensity at pH = 3.30 with a maximum diameter of 33.21 ± 12.8 μm. By pH reduction, insoluble complexes began to dissociate and dissolve as a result of the gradual protonation of carboxyl groups on the structure of HMP. Thus, the particle size reduced when the pH approached 3.00 (12.918 ± 2.48 μm) and 2.70 (9.963 ± 1.26 μm). In general, lower pH resulted in larger particle size due to the stronger attraction between NaCas and HMP, which is in line with results for turbidity.

Effect of biopolymer concentration and ratio on aggregate formation

The effects of C_T and the ratio of protein to polysaccharide on the formation of NaCas/HMP coacervate as a function of pH (2.00–7.00) were also investigated. As illustrated in Fig. 4a, turbidity increases significantly when C_T increases, and its maximum peak increase from 0.6 at 0.1% to 2.1 at 0.8%. Turbidity increased more in region C, where complex coacervates are developed. Further increases in solute amount leads to the high viscosity of the mixture, and therefore, more complexes are formed at higher C_T. It can be attributed that more counterions were easily released with increasing biopolymer concentration. It is possible that as biopolymer concentration increased, more counterions were easily released [51]. Moreover, results showed that the total concentration of NaCas and HMP did not affect the pH_c, which confirmed the assumption that soluble complexes are constituted of a certain amount of protein and a single polysaccharide molecule. As a result, pH_c is independent of the biopolymer amounts [52].

The ratio of protein/polysaccharide, i.e., the stoichiometries of the biopolymers, plays a vital role in the CC process due to its influence on the balance of macromolecule charges and affects the intensity of the electrostatic interactions between the polymers [7, 53, 54]. Therefore, the effect of the NaCas/HMP ratio from 1:1 to 8:1 (C_T = 0.4% *w/v*) on the solution turbidity as a function of pH is exhibited in Fig. 4b. It is evident that as the protein/polysaccharide ratio was reduced from 8:1 to 1:1, the pH_{max} shifted to lower pH values, and the maximum turbidity was obtained at a ratio of 4:1. Although the pH_c value (~5.70) remained unaltered, the coacervation happened at different ratios, which allowed obtaining different pH_ϕ values. Therefore, it can be concluded that pH_c is not affected by the mixing ratio, but the ratio can change $pH_{\phi 1}$. When more proteins are available per polysaccharide chain, the phase separation occurs at a higher pH, which is in agreement with previous work [1, 55]. The negatively charged groups of HMP are found in excessive amounts at pH_c, due to the limited amounts of patches

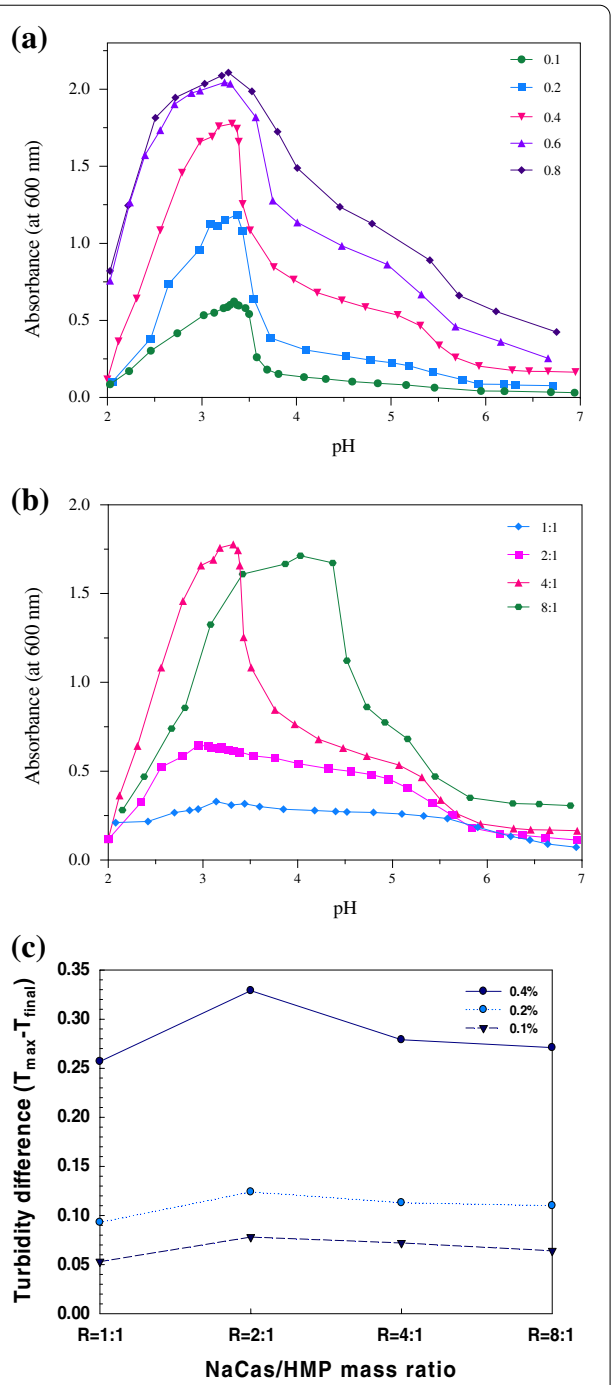

Fig. 4 Turbidity of the NaCas/HMP mixtures as a function of pH: **a** at ratio 4:1 and different C_T, **b** at $C_T = 0.4\%$ *w/v* and varying mass ratios (R = 1:1, 2:1, 4:1, 8:1), and **c** turbidity reduction of NaCas/HMP coacervates

with a positive charge in molecules of NaCas. Therefore, the pH_c value is dependent on the NaCas concentration rather than the HMP concentration. Nonetheless, at pH_ϕ, enough amounts of positively charged NaCas groups can be combined with HMP [1]. Overall, the pH_{max} was dependent on C_T, and it was also shifted from 3.00 to 3.30 by increasing the ratio from 1:1 to 8:1, discovering the interpolymer interactions are effectively enhanced [52].

At higher concentrations of polysaccharides, the assumed intra-polymeric and inter-polymeric interactions and aggregation in protein/polysaccharide mixtures declined or even stopped. Compared to protein molecules in protein/polysaccharide mixtures, the molecules of polysaccharides are of less contribution to light scattering [20]. When the protein/polysaccharide ratio declines, the nanoparticle sizes are reduced, denoting that higher concentrations of polysaccharide can safeguard more NaCas aggregates from further aggregation [40].

A plot of turbidity reduction at 10 min vs. the mass ratio of NaCas/HMP mixture is depicted to correlate the turbidity decrease with the CC of NaCas/HMP (Fig. 4c). As it was shown, the most significant turbidity reduction was achieved at R = 2:1, which is consistent with the stoichiometric ratio of coacervates identified by turbidimetry. However, there was no turbidity reduction at the other ratios. A similar ratio of 1.8:1 for Lysozyme/β-conglycinin coacervate has been obtained in the previous works [26, 56]. As a result, the degree of turbidity reduction reflected the tendency of coacervation and rearrangement, and showed that the unique turbidity reduction behavior of NaCas/HMP was meaningful. Furthermore, it can be stated that the ratio of 2:1 protein: polysaccharide (Pr:Ps) has the highest turbidity reduction, which requires further investigation in the other mixtures.

FTIR features of NaCas–HMP coacervates

FTIR analysis confirmed the electrostatic interactions between NaCas and HMP formed between amino groups of protein and carboxyl groups of HMP, as shown in Fig. 5. Polysaccharides such as pectin have a free carboxyl group that imparts a negative charge to these molecules. During CC, carboxyl groups in polysaccharides interact with amino groups in proteins to form a complex that contains amide. FT-IR analysis was carried out to confirm the formation of amide due to the interaction of free carboxyl and amino groups present in HMP and NaCas, respectively. Actually, the interactions of functional groups at the molecular level can result in new peaks and changes in the intensity or location of absorption bands (i.e., shifting) in FTIR spectra [12, 47, 57, 58].

The peaks at 1651, 1539, and 1417 cm^{-1} for NaCas belong to the amide I and II (stretching vibration of C = O, C–N, and bending vibration of N–H) absorption bands, and the signal peaks at 1647, 1224, and

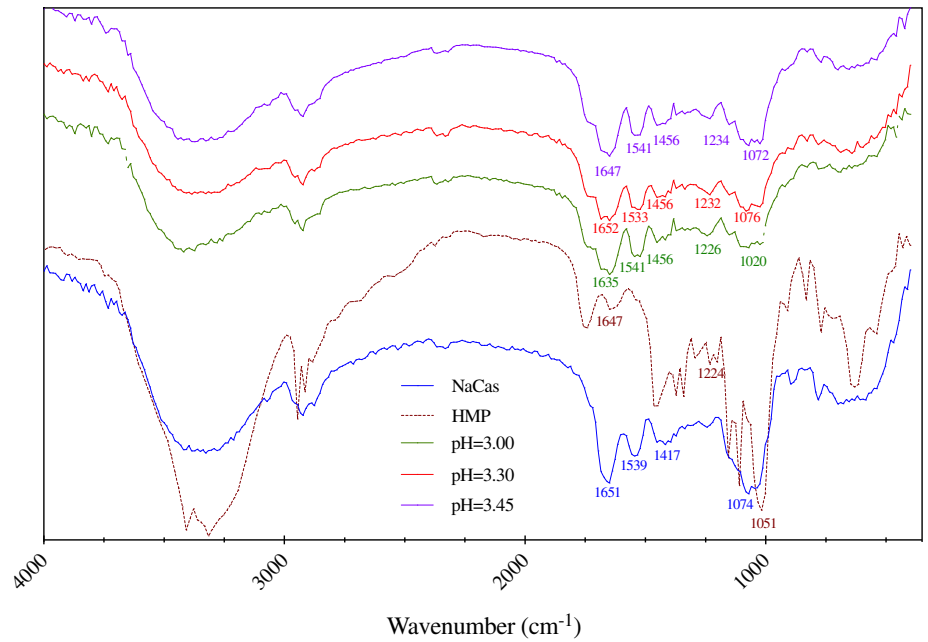

Fig. 5 FTIR spectra of NaCas, HMP (pH = 5.00) and NaCas/HMP coacervate (R = 4:1 and C_T = 0.4% *w/v*) at different pH values (3.00, 3.30, and3.45)

1051 cm^{-1} for HMP belong to the stretching vibration signals of S = O, S–O, and C–O, respectively. By coacervation at pH_{max} = 3.30, the signals at 1539 and 1417 cm^{-1} for NaCas shifted to 1533 and 1456 cm^{-1}, respectively, while the 1224 and 1051 cm^{-1} for HMP shifted to 1232 and 1076 cm^{-1}, and acidification had little change on the HMP peaks. Since no bond formation and rupture are observed for the coacervate, the covalent binding of NaCas to HMP does not exist in the coacervation system.

Thermal characteristics of coacervates

To further investigate the thermal properties of NaCas/HMP coacervates, TGA was applied as the percentage mass loss from 20 to 520 °C. As shown in Fig. 6a, approximately 5% mass loss of NaCas, HMP, and coacervates at different pH values was observed at about 200 °C, and then settled down, which can be attributed to the loss of free and bound water in the samples [59]. However, the TGA curves of NaCas and HMP showed steep loss when the temperature rose from 210 to 500 °C, but the coacervates showed a monotonous reduction in mass loss. The more sharp reduction in mass loss of HMP at about 200–280 °C relates to the carboxyl group decomposition and dehydration of saccharide rings [12]. Furthermore, the coacervates showed less weight loss below 200 °C as well as above 280 °C. In addition, less mass loss occurred for NaCas/HMP coacervate at pH 4.50.

Typical DSC graphs corresponding to NaCas, HMP, and their coacervates at different pH values are provided in Fig. 6b. Although thermographs of HMP showed endothermic processes developing at around 80, 160, and 210 °C, NaCas also showed less endothermic processes at these temperatures. The endothermic process at the first temperature within 60–90 °C was related to the intrinsic water eliminated during the process. However, the NaCas/HMP coacervates presented less endothermic properties at the same temperature range for NaCas and HMP. Consequently, the complex coacervates were inferred to have higher thermal stability compared with NaCas and HMP at temperatures below 220 °C, which is in line with the TGA results.

Rheological behaviors

It is obvious that viscosity is notably influenced by the size and composition of the aggregates (Lu et al. [62]). From the previous sections, it was found NaCas/HMP coacervate at a ratio of 4:1% w/w and C_T = 0.4% *w/v* has the maximum turbidity and particle size. Therefore, the rheological behaviors of NaCas, HMP at pH 5.00, and their coacervates at pH values of 3.00, 3.30, and 3.45 are evaluated and provided in Fig. 7. The apparent viscosity was decreased by increasing shear rate (0.1–100 s^{-1}) revealed the non-Newtonian shear-thinning behaviors. Shear-thinning characteristics of the coacervates can be related to the structural rearrangement under shear [9, 60]. It was found that a greater viscosity at pH 3.30 (~ 12 mPa.s at $\gamma = 1\ s^{-1}$) than that of the other coacervates at pH values 3.00 and 3.45 in which

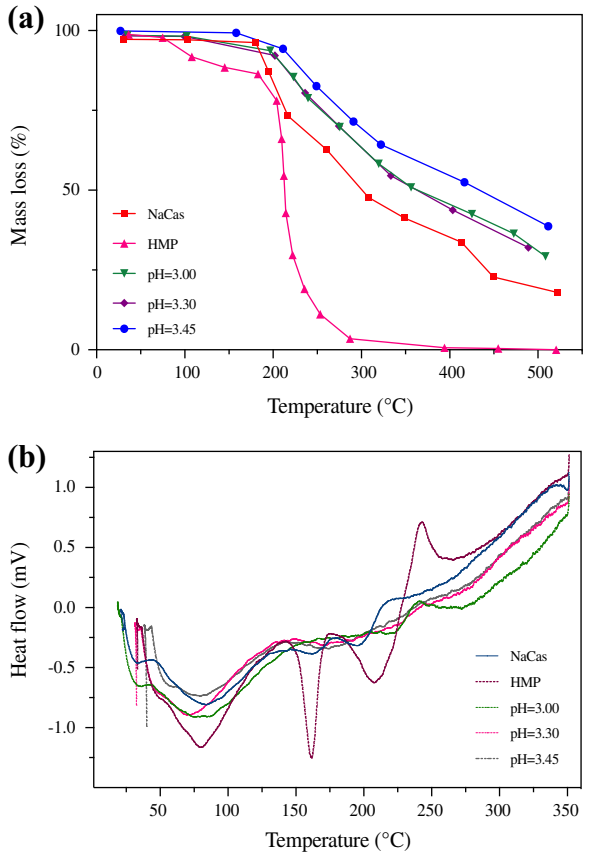

Fig. 6 Thermal behavior of NaCas, HMP, and NaCas/HMP coacervates at pH 3.00, 3.30 and 3.45. **a** Thermogravimetric analysis from 20 to 520 °C, **b** DSC Thermographs from 20 to 350 °C at heating rate 10 °C/min

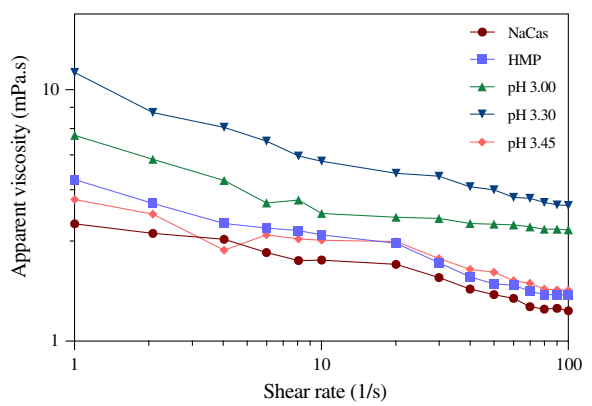

Fig. 7 Rheological behaviors of NaCas, HMP (pH = 5.00) and their coacervate at pH 3.00, 3.30, and3.45 (temperature 25 °C)

the viscosity was close to the protein or polysaccharide. Therefore, the more tightly packed structure was achieved at pH 3.30 due to the maximum electrostatic interactions between proteins and polysaccharide. On the other hand, the coacervates do not possess a completely compact structure at pH values upper or lower than the optimum pH and their formation was highly pH dependent [61]. Similar findings have been also reported for the whey protein/high metoxyl pectin and rice bran protein/flax seed gum coacervates [9, 13]. On the other hand, it can be stated that the insoluble aggregates at pH 3.45 lead to viscosity reduction through the formation of insoluble aggregates. By self-aggregation of HMP and denaturation of NaCas at lower pH values, particularly 3.30, the viscosity returns to a higher value. Similar results have been reported for the lysozyme and κ-carrageenan coacervates [62].

Microscopic observation

Optical microscopy was applied to survey NaCas and HMP at pH 5.00, and the formation of complex coacervates at pH values of 3.00, 3.30, 3.45, and 5.00 (Fig. 8). At pH = 5.00, no coacervate formation was observed. When the pH decreased to 3.45, a slight aggregation of coacervates was observed. By further reduction in pH, smaller coacervates accumulated to generate larger coacervates and create more compact structures at pH = 3.30 (pH_{max}). The aforementioned findings are in line with the results of ζ-potential, turbidity, and particle size.

Coacervation yield

Another important parameter in the optimization of the CC process is the yield of complex coacervate [53, 54]. The coacervates were obtained by mixing two biopolymers at different ratios and biopolymer concentrations of NaCas/HMP after adjusting the pH. It was considered as the amount of coacervate to the total mass of both NaCas and HMP used to prepare the dispersions, and the data are provided in Table 2. By the way, the optimized ratio (4:1) illustrated a higher yield than the other ratios ($P < 0.05$). It may be due to the decrement of soluble complexes, the increment of electrostatic interactions, and the insoluble complexes. The low yield of complex coacervate resulted from the creation of soluble complexes owing to electrostatic interactions and the delicate balance between charges [11, 54]. Results demonstrated that the highest acquired yield of coacervation was 39.8%. Although the highest amount of complex coacervates (pH_{max} = 3.00) has been obtained for sodium caseinate/low methoxyl pectin at ratio 2:1 [4], but the highest yield was achieved at pH 3.30 and R = 4:1 for NaCas/HMP, which clearly indicated the effect of esterification of the coacervate formation. Furthermore, the effect of the biopolymer mixing ratio on the coacervation yield was

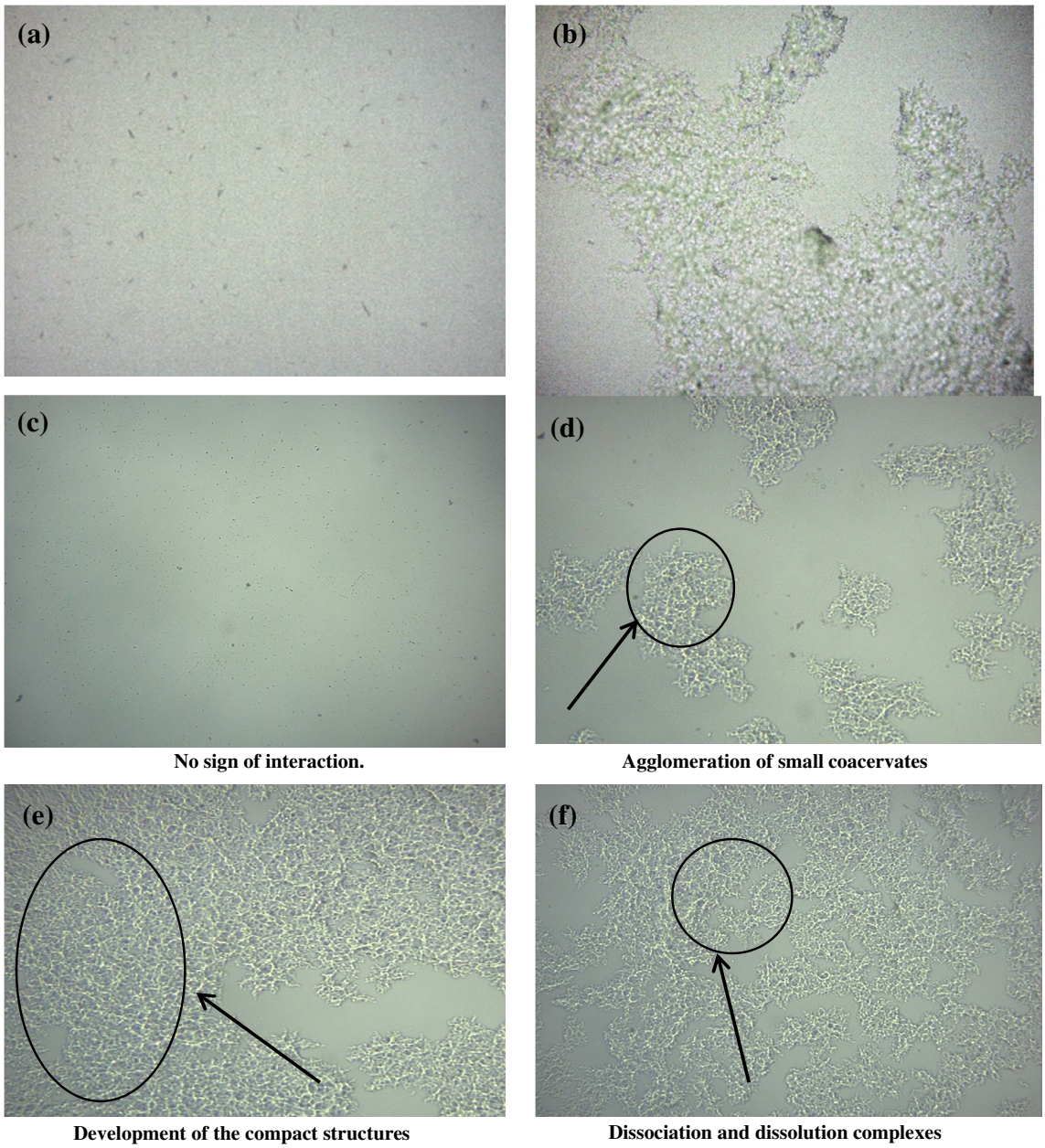

Fig. 8 Microscopic image (40x) of: **a** HMP (0.08% *w/v*) at pH = 5.00, **b** NaCas (0.32% *w/v*) at pH = 5.00, complex coacervates at; **c** pH 5.00 **d** pH 3.45, **e** pH 3.30, and **f** pH 3.00

evident; indicating the higher amount of protein used for coacervate preparation means a higher coacervation yield. Moreover, it has been found that the coacervate yield was drastically diminished at pH values below 3.5 due to a low degree of ionization of polysaccharide molecules and at pH values above 5.00 due to the low solubility of proteins [61].

Conclusion

The current study illustrated the ability of sodium caseinate (NaCas) molecules to interact with high methoxyl pectin (HMP) molecules and form soluble and insoluble complexes. Light scattering and ζ-potential measurements were used to understand the formation of the coacervates as a function of pH (2.00–7.00) and NaCas/HMP ratio. The NaCas/HMP

Table 2 Yield (%) of complex coacervates by changing the NaCas/HMP mixing ratios and biopolymer concentration*

Protein to polysaccharide ratio			
Total biopolymer concentration	**2:1**	**4:1**	**8:1**
0.1	9.26 ± 0.25^{c}	31.93 ± 0.31^{c}	27.94 ± 0.52^{c}
0.2	11.99 ± 0.27^{b}	35.93 ± 0.38^{b}	29.94 ± 0.42^{b}
0.4	18.8 ± 0.63^{a}	39.8 ± 0.66^{a}	33.43 ± 0.57^{a}

* Alphabetic letter was used to show the significant difference among the sample ($P < 0.05$)

interactions caused by acidification resulted in increasing the turbidity and decreasing ζ-potential, which was confirmed by particle size and FTIR. The maximum yield occurred at a pH of 3.30, a total biopolymer concentration of 0.4% (*w*/*v*), and a NaCas/HMP ratio of 4:1. TGA results indicated that the thermal stability of the produced complex coacervates was higher compared to each of the polymers. These results showed their importance in encapsulating bioactive compounds (such as herbal extracts) with direct applications in the food and pharmaceutical industries using NaCas/HMP complexes.

Acknowledgements
I would like to express my very great appreciation to Dr. Haghighi asl and Dr. Rafe for his valuable and constructive suggestions during the planning and development of this research work.

Author contributions
FA: data curation; investigation; methodology; and writing—original draft. AHA: conceptualization; supervision; validation; and writing—review and editing, AR: conceptualization; supervision; validation; visualization; and writing—review and editing. All authors read and approved the final manuscript.

Funding
The authors would like to thank Semnan University gratefully for providing the financial support of this project.

Availability of data and materials
All data are presented in the manuscript.

Declarations

Ethics approval and consent to participate
The authors will follow the Ethical Responsibilities of Authors and COPE rules. On behalf of all co-authors, I believe the participants are giving informed consent to participate in this study.

Consent for publication
I, Faezeh Ardestani give my consent for the submitted manuscript to be published in the Chemical and Biological Technologies in Agriculture.
II, Ali Haghighi asl give my consent for the submitted manuscript to be published in the Chemical and Biological Technologies in Agriculture.

Competing interests
The authors declare that they have no competing interests.

Received: 28 August 2022 Accepted: 1 November 2022
Published online: 08 November 2022

References

1. Wang J, Dumas E, Gharsallaoui A. Low methoxyl pectin/sodium caseinate complexing behavior studied by isothermal titration calorimetry. Food Hydrocoll. 2019;88:163–9.
2. Li GY, Chen QH, Su CR, Wang H, He S, Liu J, et al. Soy protein-polysaccharide complex coacervate under physical treatment: Effects of pH, ionic strength and polysaccharide type. Innov Food Sci Emerg Technol. 2021;68:102612.
3. Stone AK, Nickerson MT. Formation and functionality of whey protein isolate-(kappa-, iota-, and lambda-type) carrageenan electrostatic complexes. Food Hydrocoll. 2012;27:271–7.
4. Eghbal N, Saeid M, Mousavi M, Degraeve P. Complex coacervation for the development of composite edible films based on LM pectin and sodium caseinate. Carbohydr Polym. 2016;151:947–56.
5. Eghbal N, Degraeve P, Oulahal N, Yarmand MS, Mousavi ME, Gharsallaoui A. Low methoxyl pectin/sodium caseinate interactions and composite film formation at neutral pH. Food Hydrocoll. 2017;69:132–40.
6. Muhoza B, Xia S, Zhang X. Gelatin and high methyl pectin coacervates crosslinked with tannic acid: the characterization, rheological properties, and application for peppermint oil microencapsulation. Food Hydrocoll. 2019;97:105174.
7. Gee P, Gupta R, Prasad Y, Adhikari B. Optimisation of the complex coacervation between canola protein isolate and chitosan. J Food Eng. 2016;191:58–66.
8. Chen K, Zhang M, Mujumdar AS, Wang H. Quinoa protein-gum Arabic complex coacervates as a novel carrier for eugenol: Preparation, characterization and application for minced pork preservation. Food Hydrocoll. 2021;120:106915.
9. Hasanvand E, Rafe A. Rheological and structural properties of rice bran protein-flaxseed (*Linum usitatissimum* L.) gum complex coacervates. Food Hydrocoll. 2018;83:296–307.
10. Raei M, Shahidi F, Farhoodi M, Jafari SM, Rafe A. Application of whey protein—pectin nano-complex carriers for loading of lactoferrin. Int J Biol Macromol. 2017;105:281–91.
11. Timilsena YP, Wang B, Adhikari R, Adhikari B. Advances in microencapsulation of polyunsaturated fatty acids (PUFAs)-rich plant oils using complex coacervation: a review. Food Hydrocoll. 2017;69:369–81.
12. Emamverdian P, Moghaddas Kia E, Ghanbarzadeh B, Ghasempour Z. Characterization and optimization of complex coacervation between soluble fraction of Persian gum and gelatin. Colloid Surf Physicochem Eng Asp. 2020;607:125436.
13. Raei M, Rafe A, Shahidi F. Rheological and structural characteristics of whey protein—pectin complex coacervates. J Food Eng. 2018;228:25–31.
14. Jahromi M, Niakousari M, Golmakani MT, Mohammadifar MA. Physicochemical and structural characterization of sodium caseinate based film-forming solutions and edible films as affected by high methoxyl pectin. Int J Biol Macromol. 2020;165:1949–59.
15. Choi I, Han J. Development of a novel on–off type carbon dioxide indicator based on interactions between sodium caseinate and pectin. Food Hydrocoll. 2018;80:15–23.
16. Cheng W, McClements DJ. Biopolymer-stabilized conjugated linoleic acid (CLA) oil-in-water emulsions: impact of electrostatic interactions on formation and stability of pectin—caseinate—coated lipid droplets. Colloid Surf Physicochem Eng Asp. 2016;511:172–9.
17. Niu F, Su Y, Liu Y, Wang G, Zhang Y, Yang Y. Colloids and surfaces B: biointerfaces ovalbumin—gum arabic interactions: effect of pH, temperature, salt, biopolymers ratio and total concentration. Colloid Surf B Biointerfaces. 2014;113:477–82.
18. Liu J, Shim YY, Shen J, Wang Y, Reaney MJT. Whey protein isolate and flaxseed (*Linum usitatissimum* L.) gum electrostatic coacervates: turbidity and rheology. Food Hydrocoll. 2017;64:18–27.
19. Rafe A, Razavi SMA. Effect of thermal treatment on chemical structure of β-lactoglobulin and basil seed gum mixture at different states by ATR-FTIR spectroscopy. Int J Food Prop. 2015;18:2652–64.
20. Hasanvand E, Rafe A, Emadzadeh B. Phase separation behavior of flaxseed gum and rice bran protein complex coacervates. Food Hydrocoll. 2018;82:412–23.
21. Timilsena YP, Wang B, Adhikari R, Adhikari B. Preparation and characterization of chia seed protein isolate-chia seed gum complex coacervates. Food Hydrocoll. 2015;52:554–63.
22. Anema SG, de Kruif CGK. Phase separation and composition of coacervates of lactoferrin and caseins. Food Hydrocoll. 2016;52:670–7.

23. Anema SG, De Kruif CG. Interaction of lactoferrin and lysozyme with casein micelles. Biomacromol. 2011;12:3970–6.
24. Blocher McTigue WC, Voke E, Chang LW, Perry SL. The benefit of poor mixing: kinetics of coacervation. Phys Chem Chem Phys. 2020;22:20643–57.
25. Chapeau AL, Tavares GM, Hamon P, Croguennec T, Poncelet D, Bouhallab S. Spontaneous co-assembly of lactoferrin and β-lactoglobulin as a promising biocarrier for vitamin B9. Food Hydrocoll. 2016;57:280–90.
26. Zheng J, Gao Q, Ge G, Wu J, Tang C, he, Zhao M, et al. Dynamic equilibrium of β-conglycinin/lysozyme heteroprotein complex coacervates. Food Hydrocoll. 2022. https://doi.org/10.1016/j.foodhyd.2021.107339.
27. Gorji SG, Gorji EG, Mohammadifar MA. Characterisation of gum tragacanth (Astragalus gossypinus)/sodium caseinate complex coacervation as a function of pH in an aqueous medium. Food Hydrocoll. 2014;34:161–8.
28. Hasandokht Firooz M, Mohammadifar MA, Haratian P. Self-assembly of β-lactoglobulin and the soluble fraction of gum tragacanth in aqueous medium. Int J Biol Macromol. 2012;50:925–31.
29. Weinbreck F, Nieuwenhuijse H, Robijn GW, De Kruif CG. Complexation of whey proteins with carrageenan. J Agric Food Chem. 2004;52:3550–5.
30. Rodriguez Patino JM, Pilosof AMR. Protein—polysaccharide interactions at fluid interfaces. Food Hydrocoll. 2011;25:1925–37.
31. Surh J, Decker EA, Mcclements DJ. Influence of pH and pectin type on properties and stability of sodium-caseinate stabilized oil-in-water emulsions. Food Hydrocoll. 2006;20:607–18.
32. Souza CJF, da Costa AR, Souza CF, Tosin FFS, Garcia-Rojas EE. Complex coacervation between lysozyme and pectin: effect of pH, salt, and biopolymer ratio. Int J Biol Macromol. 2018;107:1253–60.
33. Tang MX, Zhu YD, Li D, Adhikari B, Wang LJ. Rheological thermal and microstructural properties of casein/κ-carrageenan mixed systems. Lwt. 2019;113:108296.
34. Xiong W, Li Y, Ren C, Li J, Li B, Geng F. Thermodynamic parameters of gelatin—pectin complex coacervation. Food Hydrocoll. 2021;120:106958.
35. Ren JN, Hou YY, Fan G, Zhang LL, Li X, Yin K, et al. Extraction of orange pectin based on the interaction between sodium caseinate and pectin. Food Chem. 2019;283:265–74.
36. Chai C, Lee J, Huang Q. The effect of ionic strength on the rheology of pH-induced bovine serum albumin/κ-carrageenan coacervates. LWT Food Sci Technol. 2014;59:356–60.
37. Plati F, Ritzoulis C, Pavlidou E, Paraskevopoulou A. Complex coacervate formation between hemp protein isolate and gum arabic: formulation and characterization. Int J Biol Macromol. 2021;182:144–53.
38. O'Kennedy BT, Mounsey JS. Control of heat-induced aggregation of whey proteins using casein. J Agric Food Chem. 2006;54:5637–42.
39. Schmitt C, Sanchez C, Desobry-Banon S, Hardy J. Critical reviews in food science and nutrition structure and technofunctional properties of protein—polysaccharide complexes: a review. Crit Rev Food Sci Nutr. 1998;38:689–753.
40. Kobori T, Iwamoto S, Takeyasu K, Ohtani T. Biopolymers volume 85/Number 4 295. Biopolymers. 2007;85:392–406.
41. Harnsilawat T, Pongsawatmanit R, McClements DJ. Characterization of β-lactoglobulin-sodium alginate interactions in aqueous solutions: a calorimetry, light scattering, electrophoretic mobility and solubility study. Food Hydrocoll. 2006;20:577–85.
42. Happi Emaga T, Garna H, Paquot M, Deleu M. Purification of pectin from apple pomace juice by using sodium caseinate and characterisation of their binding by isothermal titration calorimetry. Food Hydrocoll. 2012;29:211–8.
43. Gharanjig H, Gharanjig K, Hosseinnezhad M, Jafari SM. Development and optimization of complex coacervates based on zedo gum, cress seed gum and gelatin. Int J Biol Macromol. 2020;148:31–40.
44. Yang Y, Anvari M, Pan CH, Chung D. Characterisation of interactions between fish gelatin and gum arabic in aqueous solutions. Food Chem. 2012;135:555–61.
45. Chang C, Wang T, Hu Q, Luo Y. Zein/caseinate/pectin complex nanoparticles: formation and characterization. Int J Biol Macromol. 2017;104:117–24.
46. Maciel VBV, Yoshida CMP, Franco TT. Chitosan/pectin polyelectrolyte complex as a pH indicator. Carbohydr Polym. 2015;132:537–45.
47. Ansarifar E, Mohebbi M, Shahidi F, Koocheki A, Ramezanian N. Novel multilayer microcapsules based on soy protein isolate fibrils and high methoxyl pectin: Production, characterization and release modeling. Int J Biol Macromol. 2017;97:761–9.
48. Sanchez C, Mekhloufi G, Renard D. Complex coacervation between β-lactoglobulin and acacia gum: a nucleation and growth mechanism. J Coll Interface Sci. 2006;299:867–73.
49. Anal AK, Tobiassen A, Flanagan J, Singh H. Preparation and characterization of nanoparticles formed by chitosan—caseinate interactions. Coll Surf B Biointerfaces. 2008;64:104–10.
50. Ghasemi S, Jafari SM, Assadpour E, Khomeiri M. Nanoencapsulation of D-limonene within nanocarriers produced by pectin—whey protein complexes. Food Hydrocoll. 2018;77:152–62.
51. Niu F, Su Y, Liu Y, Wang G, Zhang Y, Yang Y. Ovalbumin-gum arabic interactions: effect of pH, temperature, salt, biopolymers ratio and total concentration. Coll Surf B Biointerfaces. 2014;113:477–82.
52. Weinbreck F, de Vries R, Schrooyen P, de Kruif CG. Complex coacervation of whey proteins and gum arabic. Biomacromol. 2003;4:293–303.
53. Wang B, Adhikari B, Barrow CJ. Optimisation of the microencapsulation of tuna oil in gelatin—sodium hexametaphosphate using complex coacervation. Food Chem. 2014;158:358–65.
54. Bakry AM, Huang J, Zhai Y, Huang Q. Myofibrillar protein with κ- or λ-carrageenans as novel shell materials for microencapsulation of tuna oil through complex coacervation. Food Hydrocoll. 2019;96:43–53.
55. Lv Y, Yang F, Li X, Zhang X, Abbas S. Formation of heat-resistant nanocapsules of jasmine essential oil via gelatin/gum arabic based complex coacervation. Food Hydrocoll. 2014;35:305–14.
56. Zheng J, Gao Q, Ge G, Wu J, Tang CH, Zhao M, et al. Heteroprotein complex coacervate based on β-Conglycinin and lysozyme: dynamic protein exchange, thermodynamic mechanism, and lysozyme activity. J Agric Food Chem. 2021;69:7948–59.
57. Saravanan M, Rao KP. Pectin—gelatin and alginate-gelatin complex coacervation for controlled drug delivery: influence of anionic polysaccharides and drugs being encapsulated on physicochemical properties of microcapsules. Carbohydr Polym. 2010;80:808–16.
58. Milošević MM, Đorđević TR, Antov MG. Complex coacervation of acid-extracted fiber from butternut squash (Cucurbita moschata) and protein. Food Hydrocoll. 2020. https://doi.org/10.1016/j.foodhyd.2020.105999.
59. Li Y, Zhang X, Sun N, Wang Y, Lin S. Formation and evaluation of casein-gum arabic coacervates via pH-dependent complexation using fast acidification. Int J Biol Macromol. 2018;120:783–8.
60. Wee MSM, Nurhazwani S, Tan KWJ, Goh KKT, Sims IM, Matia-Merino L. Complex coacervation of an arabinogalactan—protein extracted from the *Meryta sinclarii* tree (puka gum) and whey protein isolate. Food Hydrocoll. 2014;42:130–8.
61. Espinosa-Andrews H, Báez-González JG, Cruz-Sosa F, Vernon-Carter EJ. Gum arabic-chitosan complex coacervation. Biomacromoleculers. 2007;8:1313–8.
62. Lu X, Xie S, Wang L, Xie H, Lei Q, Fang W. Electrostatic-driven structural transformation in the complexation of lysozyme and κ-carrageenan. Chem Phys. 2020;538:110910.

Publisher's Note